JOURNAL OF SPACECRAFT AND ROCKETS
Vol. 31, No. 1, January–February 1994

Engineering Notes

ENGINEERING NOTES are short manuscripts describing new developments or important results of a preliminary nature. These Notes cannot exceed 6 manuscript pages and 3 figures; a page of text may be substituted for a figure and vice versa. After informal review by the editors, they may be published within a few months of the date of receipt. Style requirements are the same as for regular contributions (see inside back cover).

Engineering Code for Hypersonic Vehicle Optimization

Richard A. Thompson* and Christopher J. Riley†
NASA Langley Research Center, Hampton, Virginia 23681

Introduction

OPTIMIZATION of complex systems, such as aerospace vehicles, crosses many disciplinary boundaries and is still a relatively new field of engineering research. Although full multidisciplinary optimization of these systems is the ultimate goal and progress toward these ends has been made,[1,2] optimization within a single discipline remains an important component. Development of optimization techniques in fields such as structural mechanics and design has been well published,[3,4] but examples of aerodynamic optimization have been less visible. This is especially true when considering the hypersonic flight regime, although some work has been recently reported.[5–7]

Optimization algorithms have existed for years but the integration of detailed simulation codes with these algorithms has generally been cost prohibitive. The high computational demands of fluid dynamic simulation is obviously the major contributor to a lack of applications in aerodynamic optimization. The use of approximate engineering codes in place of detailed computational fluid dynamic codes can relieve some of these limitations and can be employed to produce useful results. These codes also serve nicely for design studies due to their approximate nature and minimal computational requirements. This Note demonstrates the integration of one such approximate engineering code with a simple optimizer to demonstrate the feasibility of the method and to lay the basis for future applications.

Approximate Engineering Code: THINBL

In 1990, Riley and DeJarnette[8] presented an approximate three-dimensional inviscid technique for vehicles with spherically and elliptically blunted noses. This technique was shown to be more accurate than modified Newtonian theory and have a wider range of applicability than the axisymmetric Maslen method,[9,10] which have been two of the more popular approaches used for approximate solutions. In their inviscid technique, two stream functions that approximate the actual stream surfaces in the shock layer are coupled with a modified form of the Maslen second-order pressure equation. The resulting method is an inverse one where the shock shape is varied until the correct body shape is produced. This inverse solution is handled differently in the subsonic blunt-nose region than on the supersonic afterbody. In the former, the bow shock is fit to discrete points by conic sections, blended meridionally, and then globally iterated to match the body surface. On the afterbody, the scheme is well posed to march the shock surface downstream by extrapolation followed by local iteration to obtain the correct shape. Overall, the technique is capable of producing reasonably accurate solutions in a fraction of the time required by full solution of the inviscid Euler equations.

To predict the viscous flowfield in the approximate engineering code, Riley and DeJarnette[11] used the axisymmetric analog concept to simplify the three-dimensional boundary-layer analysis. In this approximation, the boundary-layer equations are written in streamline coordinates in which the crossflow velocity component is assumed to be zero. By substituting the streamline distance for surface distance and axisymmetric radius for the coordinate metric, the equations reduce to an axisymmetric form and can be solved by simple means. Calculation of surface streamlines for the axisymmetric analog can be done using either the surface pressure distribution or the velocity components computed from the approximate inviscid solution. It was found that the streamlines were most accurate when calculated from the surface pressure, and so appropriate transformations and integration of the momentum equation were developed. In the final methodology, these streamlines are computed as part of the inviscid solution and provide the necessary information for the boundary-layer analysis.

A set of convective heating relations developed by Zoby et al.[12] was employed in the THINBL code as reported in Ref. 11. These relations are valid for laminar and turbulent, perfect gas or equilibrium air flows. Edge conditions for the boundary-layer solution are obtained by interpolation in the inviscid solution at a distance from the wall equal to the boundary-layer thickness. Sources are cited in Ref. 12 that show this technique to compare favorably with detailed calculations at wind-tunnel and flight conditions including cases where the effects of entropy layer swallowing are important.

From an optimization standpoint, the global aerodynamic/aerothermodynamic properties of a vehicle, such as total drag and integrated heating, are equally important as the surface distributions usually presented. To illustrate the capability of the approximate method in this regard, the THINBL code was applied for the laminar, perfect gas flow over a 5-deg sphere cone at zero incidence. Freestream conditions were at Mach 15 flight and 150,000-ft (42.75-km) altitude. Calculations were performed using two nose radii, 1.5 and 9 in., to match solutions obtained using a viscous shock-layer method (VSL3D) and published in Ref. 13. These cases were part of a parametric study to investigate the effects of nose bluntness on slender conical vehicles when the body angle and base area remained fixed. It is important to note that the larger nose radius produces a flowfield which is dominated by nose bluntness whereas the small radius yields sharp cone flow over most of the afterbody. Comparison of results between the approximate and detailed solutions is shown in Table 1 where the individual drag components (pressure C_{D_p} and friction C_{D_f}), total drag coefficient C_D, and total integrated heating Q are tabulated. The approximate THINBL results compare favorably with the detailed values and support the use of the approximate code for optimization studies under similar conditions. Again, note that this is true for both nose-radii cases where the flowfields are significantly different in nature.

Optimization Example

Many optimization algorithms exist in the literature and most are simple to apply; however, this simplicity does not guarantee success because of the highly nonlinear nature of most engineering designs. A majority of the methods developed to date are based on either the minimization or maximization of a single objective function given a set of design variables or parameters. Most real problems are multicriteria in nature, and techniques in this area are not

Received March 4, 1993; revision received March 15, 1993; accepted for publication March 15, 1993.

*Aero-Space Technologist, Aerothermodynamics Branch, Space Systems Division. Senior Member AIAA.

†Aero-Space Technologist, Aerothermodynamics Branch, Space Systems Division. Member AIAA.

as advanced. When these criteria are dependent on multiple disciplines, the problem is compounded further.

If the scope is limited to a single discipline (aerodynamics/aerothermodynamics in this case), then specific examples of optimization are easier to obtain and understand. This is the approach taken here as a first step toward larger optimization problems. Specifically, it is desired to integrate an approximate hypersonic flow code with an optimizing routine as a demonstration of its feasibility and potential. The approximate flow code which enabled this work was described previously. Coupling this code with an optimizing routine is discussed next.

A pattern search method based on the work by Hook and Jeeves[14] was used as the optimizer in the current work. Although many newer and more sophisticated techniques exist, this method is straightforward, easily implemented, and has good convergence traits. It also has the benefit of not requiring derivative information from the objective function, which can be important when computer flow codes are required to supply the gradients. The disadvantage is that convergence of the method is generally slower than gradient-based techniques, and so there is a tradeoff to be made. Further study of the various techniques would be needed to determine the "optimum" optimizer although this is most likely problem dependent as well.

The Hooke and Jeeves method is used to find the minimum of a multivariable, unconstrained function of the form

$$F(\bar{x}) = F(x_1, x_2, \ldots, x_n)$$

where the x_i are the design variables. In the algorithm, a base point in the feasible space is chosen to begin the search. From there, an exploration step is taken in each of the coordinate (design variable) directions. If a better point is found from this exploration, then a new base point is established, and a pattern search is done. This pattern search is simply an extrapolation along the line between the previous and new base points. Mathematically, this extrapolation is

$$x_{i,0}^{(k+1)} = x_i^{(k+1)} + \alpha(x_i^{(k+1)} - x_i^k)$$

where $x_{i,0}$ is a new temporary base point, k the step counter, and α a factor greater than 1.0 which accelerates the search toward the optimum region. An exploration step is repeated at the temporary base point, and, if a better solution is found, then another pattern search is performed. If no better point is found after an exploration and pattern search, then the previous best point is recalled, the exploration step size is decreased, and the whole algorithm is repeated. Convergence is obtained when the exploration step size is decreased below some predefined tolerance.

As an example of this method, the approximate engineering code was coupled with the optimizing procedure to calculate minimum drag and minimum heat-load nose shapes for a 5-deg conical body with a 3.2808-ft (1-m) base radius. Conditions were the same as used previously; namely, flight at Mach 15 and 150,000-ft (42.75-km) altitude with laminar flow and perfect gas assumptions. In all cases, the base radius and cone angle remained fixed whereas the body length varied with changes in the nose radius and shape.

Table 1 Comparison of global aerodynamic/ aerothermodynamic predictions

r_n, ft	Code	C_{D_p}	C_{D_f}	C_D	Q, Btu/s
0.125	VSL3D	0.01771	0.00472	0.02243	9804
	THINBL	0.01742	0.00454	0.02197	9252
0.75	VSL3D	0.01856	0.00358	0.02213	8389
	THINBL	0.01854	0.00374	0.02228	8566

Table 2 Optimization results

Case	b	r_n, ft	C_D	Q, Btu/s
Minimum drag	0.697	0.129	0.02594	1225.74
Minimum heating	2.0 [a]	0.696	0.04381	1063.85
Both	1.729	0.285	0.02660	1165.55

[a]Limited by constraint boundary.

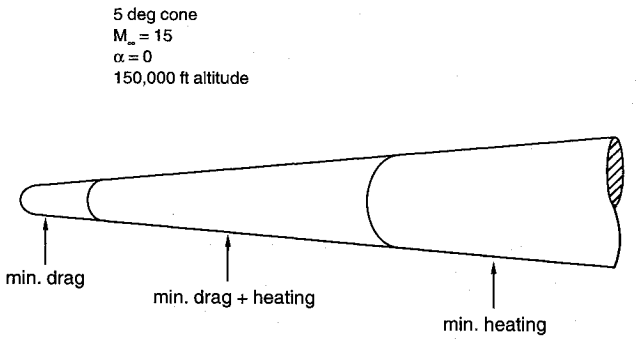

Fig. 1 Optimized nose shapes.

The geometry of the nose region is defined in THINBL by the equation

$$By^2 + z^2 = 2x - bx^2$$

where B is a parameter governing ellipticity of the cross section; x, y, and z are the Cartesian body coordinates nondimensionalized by the nose radius r_n; and b is a parameter defining the nose shape. For the present example, the body was axisymmetric such that $B=1$ which reduces the equation to

$$y^2 + z^2 = r^2 = 2x - bx^2$$

In this form, r is the local body radius and x is the axial coordinate. From this definition, the parameter b can be used to vary the nose shape from an ellipse ($b > 1$) to a hyperbola ($b < 0$). Other intermediate shapes include a sphere ($b = 1$) and a parabola ($b = 0$). The stagnation-point radius of curvature r_n completes the geometry definition. These two parameters (b and r_n) were selected as design variables to demonstrate the optimization process. A direct constraint was placed on the problem using a penalty function approach such that $b \leq 2.0$. The problem was also indirectly constrained by the analytic description of the geometry. Convergence of the design variables to within 10^{-6} was achieved by the optimizer with roughly 150 objective function calls and required approximately 5 min of computing time on a midrange workstation in each case. It should be noted that this tolerance was reached within 5% with only half as many calls illustrating the rapid convergence of the method to the optimum region.

Table 2 summarizes the results obtained with the integrated procedure. The table lists the optimum values obtained for the shape parameter and nose radius along with the computed drag and integrated heating for the cases of minimum drag, minimum total heating, and a combination of those two designs. A pictorial view of the optimized nosetips is shown in Fig. 1.

For the case of minimum drag, Table 2 (and Fig. 1) shows that the optimum nose tends toward a sharp cone (small nose radius) as would be expected. However, a finite bluntness is found that minimizes the drag because the pressure overexpansion on the conical flank yields lower wave and friction drag than for an equivalent sharp cone. Blunter nose shapes (larger b and r_n) enhance the overexpansion effect but the benefit is offset by increased pressure drag in the stagnation and shoulder regions. This effect is beneficial for minimum heating as shown for the second case where the optimum moves toward these larger nose shapes. In fact, the optimum shape was found at the b constraint boundary as noted in the table and would be larger without this constraint. Although the larger effective radius naturally reduces the stagnation heating, the main benefit was still found to be lower heating over the afterbody

because of the overexpansion. Tests with longer body geometries show that a limit on bluntness is reached when the area of the stagnation region becomes sufficiently large.

In the final optimization case, a multicriteria problem was considered which attempts to minimize both the total drag and the total heating load. This result was generated using a global criterion method which minimizes the function given by

$$F(\bar{x}) = \sum_{i=1}^{k} \frac{f_i^0 - f_i(\bar{x})}{f_i^0}$$

where the f_i^0 are the minimum drag and minimum heating values obtained in the two previous cases. In essence, this function measures the closeness of the result to the ideal solution where both drag and heating are a minimum. As expected, the nose geometry falls between the two optimum shapes identified previously in terms of shape b and radius r_n. Comparing the drag and heating values with the previous cases, it is worth noting that the result presents a good compromise between the two competing requirements.

This last case simulates most real applications in that its goals are multicriteria in nature. Additional solutions could be performed with these criteria where the weighting between minimum drag and minimum heating is varied such that a family of shapes is generated. Thus, optimization would have done its part to determine the feasible solutions and it is left to the engineer to choose among them based on the design requirements.

Concluding Remarks

Advances in computational methods and approximations for fluid flow simulation have enabled a new field of engineering application, namely, aerodynamic/aerothermodynamic optimization of flight vehicles. The use of optimization techniques coupled with computer simulations has shown promise in enhancing the usual parametric-variation type studies historically performed in wind-tunnel and computational investigations of new vehicle designs. This study demonstrated the integration of one such flowfield code with an optimizing routine to produce a useful engineering tool. Extensions to more complex shapes and a greater range of design parameters are areas requiring further study.

References

[1]Sobieszczanski-Sobieski, J., "Sensitivity Analysis and Multidisciplinary Optimization for Aircraft Design: Recent Advances and Results," *Journal of Aircraft*, Vol. 27, No. 12, 1990, pp. 993–1001.

[2]Coen, P. G., Sobieszczanski-Sobieski, J., and Dollyhigh, S. M., "Preliminary Results from the High-Speed Airframe Integration Research Project," AIAA Paper 92-1004, Feb. 1992.

[3] Haftka, R. T., Gurdul, Z., and Kamat, M. P., *Elements of Structural Optimization*, 2nd ed., Kluwer, Dordrecht, The Netherlands, 1990.

[4] Gero, J. S. (ed.), *Design Optimization*, 1st ed., Vol. 1, Academic, Orlando, FL, 1985.

[5]Dulikravich, G. S., and Sheffer, S. G., "Aerodynamic Shape Optimization of Arbitrary Hypersonic Vehicles," *Proceedings of the Third International Conference on Inverse Design Concepts and Optimization in Engineering Sciences*, edited by G. S. Dulikravich, Washington, DC, 1991, pp. 347–358.

[6]McQuade, P. D., Eberhardt, S., and Livne, E., "Optimization of a 2D Scramjet-Vehicle Using CFD and Simplified Approximate Flow Analysis Techniques," AIAA Paper 92-3673, July 1992.

[7]Lewis, M., "Propulsion/Airframe Integration for Hypersonic Waveriders," AIAA Paper 92-0304, Jan. 1992.

[8]Riley, C. J., and DeJarnette, F. R., "An Approximate Method for Calculating Three-Dimensional Inviscid Hypersonic Flow Fields," NASA TP-3018, Aug. 1990.

[9]Maslen, S. H., "Inviscid Hypersonic Flow Past Symmetric Bodies," *AIAA Journal*, Vol. 2, No. 6, 1964, pp. 1055–1061.

[10]Maslen, S. H., "Asymmetric Hypersonic Flow," NASA CR-2123, Sept. 1972.

[11]Riley, C. J., and DeJarnette, F. R., "Engineering Aerodynamic Heating Method for Hypersonic Flow," *Journal of Spacecraft and Rockets*, Vol. 29, No. 3, 1992, pp. 327–334.

[12]Zoby, E. V., Moss, J. N., and Sutton, K., "Approximate Convective-Heating Equations for Hypersonic Flows," *Journal of Spacecraft and Rockets*, Vol. 18, No. 1, 1981, pp. 64–70.

[13]Thompson, R. A., Zoby, E. V., Wurster, K. E., and Gnoffo, P. A., "An Aerothermodynamic Study of Slender Conical Vehicles," *Journal of Thermophysics and Heat Transfer*, Vol. 3, No. 4, 1989, pp. 361–367.

[14]Hooke, R., and Jeeves, T. A., "Direct Search Solution of Numerical and Statistical Problems," *Journal of the Association for Computing Machinery*, Vol. 8, No. 2, 1961, pp. 212–229.